Supplementary Material
For

Understanding complex chiral plasmonics

Xiaoyang Duan, Song Yue, and Na Liu*
Max Planck Institute for Intelligent Systems, Heisenbergstrasse 3, D-70569 Stuttgart, Germany
**To whom the correspondence should be addressed. E-mail: laura.liu@is.mpg.de*

Structure fabrication

Samples are fabricated using two-step electron-beam lithography (EBL). First, a structural layer composed of disk pairs, bars, and alignment markers are defined in a double layer PMMA resist (Allresist) using EBL (Raith e_line) on a quartz glass substrate (Suprasil, Heraeus). A 3 nm chromium adhesion layer and a 40 nm gold film are deposited on the substrate using thermal evaporation followed by a lift-off procedure. Next, a 70 nm PC403 (JCR, Japan) layer is coated on the substrate. A prebaking process is first carried out to remove the solvent from the polymer by increasing the baking temperature from 90 °C to 130 °C. A longer baking process at 180 °C for 30 min is then applied. Subsequently, the substrate is coated with a PMMA layer. Computer-controlled alignment using the gold markers is carried out to define a second structural layer composed of disk pairs. Finally, metal evaporation, lift-off, and planarization using PC403 are performed. All samples have a total area of 30 μm × 30 μm.

Optical characterization

The spectra are measured using a Fourier-transform infrared spectrometer (Bruker Vertex 80, tungsten lamp) equipped with an infrared microscope (Bruker Hyperion, numerical aperture NA = 0.4). An infrared polarizer and a broadband (700 nm – 2500 nm) infrared quarterwave plate (B. Halle Nachfl., Berlin) are used to generate incident circularly polarized light. The measured

spectra are normalized with respect to that of the substrate.

Numerical simulations

Numerical simulations are carried out using commercial software COMSOL Multiphysics based on a finite element method (FEM). The refractive indices of the quartz substrate and PC403 are taken both as 1.5. The dielectric constants of bulk gold in the near infrared region is described by the Drude model with $\omega_P = 2\pi \times 2.175 \times 10^{15} s^{-1}$, and $\gamma = 2\pi \times 6.5 \times 10^{12} s^{-1}$. Owing to the surface scattering and grain boundary effects in the thin gold film, the simulation results are obtained using a damping constant that is three times larger than the bulk value.

Transmittance spectra of the gold bar

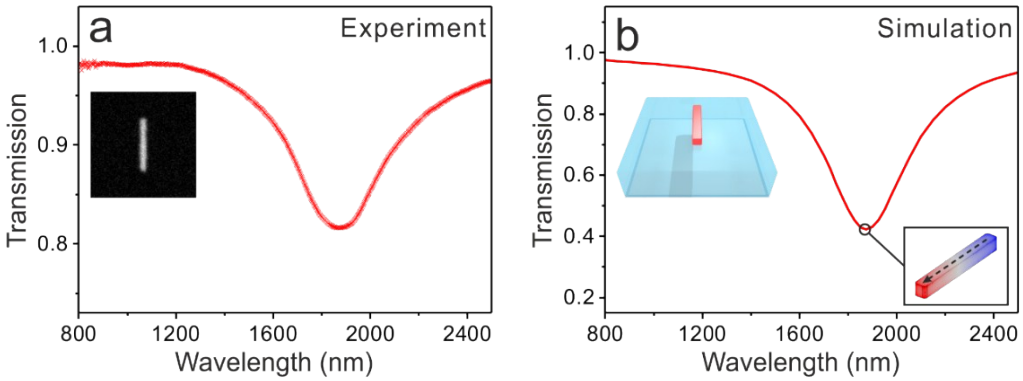

Figure S1: (a) Experimental and (b) simulated CD spectra of the plasmonic achiral molecule. Charge distribution at the resonance (~1900 nm) is included as the inset image in (b).

Analytical model

Here, we develop an extended plasmonic Bohn Kuhn model[S1,S2]. Taking the superstructures in Fig. 5 as an example, the L-modes of the two disk pairs on the upper and bottom layers can be

represented by a yellow L-oscillator ($u_1 = A_1 e^{-i\omega t}$) and a blue L-oscillator ($u_2 = A_2 e^{-i\omega t}$), respectively (see Fig. 5c). The T-modes of the two disk pairs are represented by a yellow T-oscillator ($u_4 = A_4 e^{-i\omega t}$) and a blue T-oscillator ($u_5 = A_5 e^{-i\omega t}$), respectively. In each disk pair, the L-mode and the T-mode oscillate perpendicularly to each other. The gold bar is represented by a red oscillator ($u_3 = A_3 e^{-i\omega t}$). The superstructure interacts with circularly polarized light propagating along the z-direction. The coupled oscillators fulfill the following Lorentzian equations,

$$\begin{bmatrix} D_1 & \kappa_{12} & \kappa_{13} & & \\ \kappa_{12} & D_2 & 0 & \ddots & \\ \kappa_{13} & 0 & D_3 & & \\ & \ddots & & D_4 & \kappa_{45} \\ & & & \kappa_{45} & D_5 \end{bmatrix} \begin{bmatrix} A_1 \\ A_2 \\ A_3 \\ A_4 \\ A_5 \end{bmatrix} = - \begin{bmatrix} g_1 E_y e^{ik(z+d/2)} \\ g_2 E_x e^{ik(z-d/2)} \\ g_3 E_x e^{ik(z-d/2)} \\ g_4 E_x e^{ik(z+d/2)} \\ g_5 E_y e^{ik(z-d/2)} \end{bmatrix} \quad (1)$$

where $D_i = \left(\omega_{0i}^2 - \omega^2 - i\omega\gamma_i\right), i = 1,2,\cdots,5$. ω_{0i} is the resonance frequency; γ_i is the loss in the oscillator; κ_{12}, κ_{13}, and κ_{45} denote the corresponding coupling constants of two coupled oscillators. The vertical distance between the two layers is d; g_i is a geometrical parameter indicating how strong the mode is coupled to the external field.

Equation 1 consists of two independent subsystems. The solution to the first subsystem can be obtained,

$$A_1 = - \frac{g_1 E_y e^{ikd/2} - \left(g_2 \frac{\kappa_{12}}{D_2} + g_3 \frac{\kappa_{13}}{D_3}\right) E_x e^{-ikd/2}}{D_1 - \frac{\kappa_{12}^2}{D_2} - \frac{\kappa_{13}^2}{D_3}} e^{ikz} \quad (2a)$$

$$A_2 = \frac{-g_2 E_x e^{ik(z-d/2)} - \kappa_{12} A_1}{D_2} \quad (2b)$$

$$A_3 = \frac{-g_3 E_x e^{ik(z-d/2)} - \kappa_{13} A_1}{D_3} \tag{2c}$$

We assume that there are N_0 charge carriers per unit volume. By using the general formula for the current density at point r: $J(r) = -ev\delta(r)$, here $-e$ and v are the charge and velocity, respectively. The total current density can be calculated by

$$J_x = -eN_0\left(g_2\frac{du_2}{dt} + g_3\frac{du_3}{dt}\right) \tag{3a}$$

$$J_y = -eN_0\left(g_1\frac{du_1}{dt}\right) \tag{3b}$$

J_z is zero. Then, through $P(\omega,r) = J(\omega,r)/(-i\omega)$, we can derive the nonzero polarization components,

$$P_x = eN_0\left[\left(\frac{g_2^2}{D_2} + \frac{g_3^2}{D_3}\right)E_x - \frac{\left(g_2\frac{\kappa_{12}}{D_2} + g_3\frac{\kappa_{13}}{D_3}\right)g_1 E_y e^{ikd} - \left(g_2\frac{\kappa_{12}}{D_2} + g_3\frac{\kappa_{13}}{D_3}\right)^2 E_x}{\left(D_1 - \frac{\kappa_{12}^2}{D_2} - \frac{\kappa_{13}^2}{D_3}\right)}\right]e^{ikz} \tag{4a}$$

$$P_y = eN_0\left[\frac{g_1^2 E_y - g_1\left(g_2\frac{\kappa_{12}}{D_2} + g_3\frac{\kappa_{13}}{D_3}\right)E_x e^{-ikd}}{D_1 - \frac{\kappa_{12}^2}{D_2} - \frac{\kappa_{13}^2}{D_3}}\right]e^{ikz} \tag{4b}$$

Because $d \ll \lambda$, an approximation, $e^{\pm ikd} \cong 1 \pm ikd$ can be utilized.

Considering the first-order approximation of the linear constitutive equation[S3],

$$P_i(\omega) = \frac{1}{4\pi}\left\{\sum_{j=x,y,z}[\varepsilon_{ij}(\omega) - \delta_{ij}]E_j(\omega) + \sum_{j=x,y,z}\sum_{n=x,y,z}\Gamma_{ijn}(\omega)\frac{\partial E_j(\omega)}{\partial r_n}\right\} \tag{5}$$

Here, δ_{ij} is the Kronecker delta symbol, ε_{ij} is a material permittivity tensor, and Γ_{ijn} is a material

nonlocality tensor. By comparing Eq. 4 with Eq. 5, we can obtain the nonzero components of the nonlocality tensor,

$$\Gamma_{xyz} = -\Gamma_{yxz} = -4\pi e N_0 d\left[\frac{g_1\left(g_2\frac{\kappa_{12}}{D_2}+g_3\frac{\kappa_{13}}{D_3}\right)}{D_1-\frac{\kappa_{12}^2}{D_2}-\frac{\kappa_{13}^2}{D_3}}\right] \tag{6}$$

In an isotropic medium, when considering the propagation direction, we obtain

$$\Gamma = \Gamma_{xyz} = -4\pi e N_0 d\left[\frac{g_1\left(g_2\frac{\kappa_{12}}{D_2}+g_3\frac{\kappa_{13}}{D_3}\right)}{D_1-\frac{\kappa_{12}^2}{D_2}-\frac{\kappa_{13}^2}{D_3}}\right] \tag{7a}$$

Now only the first subsystem of Eq.1 is considered. Similarly, the contribution from the transvers modes can be obtained,

$$\Gamma = \Gamma_{xyz} = -4\pi e N_0 d\left[\frac{g_1\left(g_2\frac{\kappa_{12}}{D_2}+g_3\frac{\kappa_{13}}{D_3}\right)}{D_1-\frac{\kappa_{12}^2}{D_2}-\frac{\kappa_{13}^2}{D_3}}+\frac{g_4\left(g_5\frac{\kappa_{45}}{D_5}\right)}{D_4-\frac{\kappa_{45}^2}{D_5}}\right] \tag{7b}$$

The ellipticity of the propagation wave per length unit can be determined by[S3]

$$\sin 2\eta = \tanh\left[\frac{\omega^2}{c^2} Im\{\Gamma\}\right] \tag{8}$$

because $\eta \ll 1$, we can take the first-order approximation

$$\eta = \frac{\omega^2}{2c^2} Im\{\Gamma\} \tag{9}$$

Transmittance (T) can be calculated from the relation with Extinction (Ext): $Ext + T = 1$, namely,

$$\Delta Ext = Ext_{LCP} - Ext_{RCP} = T_{RCP} - T_{LCP} \tag{10}$$

From the following relation[S4],

$$\tan\eta = \frac{E_{RCP} - E_{LCP}}{E_{RCP} + E_{LCP}} = \frac{\sqrt{T_{RCP}} - \sqrt{T_{LCP}}}{\sqrt{T_{RCP}} + \sqrt{T_{LCP}}} \tag{11}$$

where E_{RCP} and E_{LCP} are the amplitudes of the right- and left- handed circularly polarized light, we can obtain $\eta = \frac{T_{RCP} - T_{LCP}}{4}$ because $\eta \ll 1$.

Finally, by substituting Eq. 9 to Eq. 11, we obtain

$$\Delta T = T_{RCP} - T_{LCP} = \frac{4\omega^2}{2c^2} Im\left\{ -4\pi e N_0 d\left[\frac{g_1\left(g_2\frac{\kappa_{12}}{D_2} + g_3\frac{\kappa_{13}}{D_3}\right)}{D_1 - \frac{\kappa_{12}^2}{D_2} - \frac{\kappa_{13}^2}{D_3}} + \frac{g_4\left(g_5\frac{\kappa_{45}}{D_5}\right)}{D_4 - \frac{\kappa_{45}^2}{D_5}} \right] \right\} \tag{12}$$

To provide a quantitative description, we use Eq. 12 to fit the simulated CD spectra in Fig. 5. The extracted parameters are $\omega_{01} = \omega_{02} = 271.8\,THz$, $\omega_{03} = 158.6\,THz$, $\omega_{04} = \omega_{05} =$ 348.6 THz; $\gamma_1 = \gamma_2 = 240\,THz$, $\gamma_3 = 120\,THz$;, $\gamma_4 = \gamma_5 = 190\,THz$, $\kappa_{12} = 4 \times 10^{28} s^{-2}$, $\kappa_{13} = 3 \times 10^{28} s^{-2}$, $\kappa_{45} = 5 \times 10^{28} s^{-2}$. For the fitting curve of Fig. 5 (i), $g_1 = g_2 = 1$, $g_3 = 1$.9, $g_4 = g_5 = 0.4$; for Fig. 5(ii), $g_1 = -g_2 = 1$, $g_3 = 1$.9, $g_4 = -g_5 = 0.4$; for Fig. 5 (iii), $g_1 = -g_2 = 1$, $g_3 = -1$.9, $g_4 = -g_5 = 0.4$. As shown in Fig. 5d, the fitted CD spectra can reproduce the experimental and simulated results very well.

Sketch of the L- and T-modes

The L- and T-modes of the four disk structures form chiral configurations of different handedness.

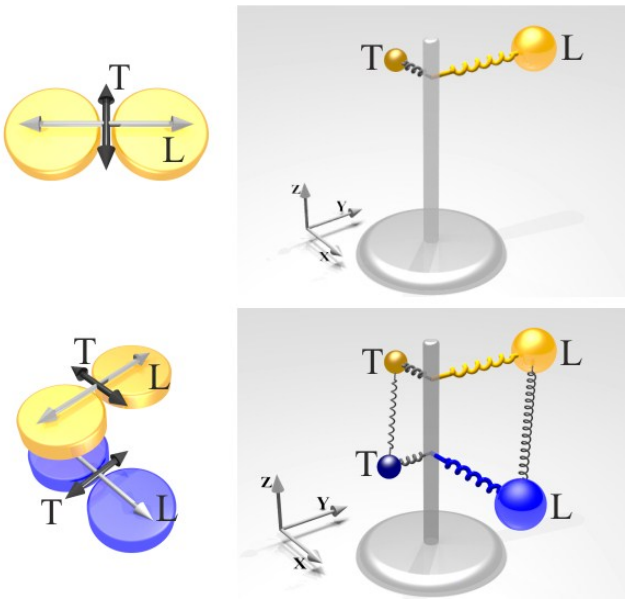

Figure S2: Illustrations for the L- and T-modes in the disk dimer and four disk structures.

Supporting Information References

S1. Bohn, M. *Phys. Z.* **1915**, *16*, 251−258.
S2. Kuhn, W. *Z. Phys. Chem. B* **1929**, *4*, 14−36.
S3. Svirko, Y. P.; Zheludev, N. I. *Polarization of Light in Nonlinear Optics*; John Wiley & Sons: New York, 1998.
S4. Fasman, G. D. *Circular Dichroism and the Conformational Analysis of Biomolecules*; Springer: New York, 1996.